INT. J. REMOTE SENSING, 2002, VOL. 23, NO. 11, 2283–2292

A curve-theorem based approach for change detection and its application to Yellow River Delta

T. X. YUE*, S. P. CHEN*, B. XU†, Q. S. LIU*, H. G. LI*, G. H. LIU*, and Q. H. YE*

*State Key Laboratory of Resources and Environment Information System, Chinese Academy of Sciences, 917 Building, Datun, Anwai, 100101 Beijing, P. R. China, e-mail: yue@lreis.ac.cn

†Center for Assessment and Monitoring of Forest and Environmental Resources (CAMFER), 151 Hilgard Hall, University of Calfornia, Berkeley, CA 94720-3110

(*Received 31 May 2000; in final form 18 June 2001*)

Abstract. A curve-theorem based approach is proposed and is used to handle NDVI data. The curve-theorem based approach includes a general index *CD* and two nonlinear transformations *SAV* and *CAV*. It is applied to Landsat MSS images of the Yellow River Delta, taken on 1 December, 1976 and 3 December, 1988. Results show that *CD* can describe the general situation of vegetation cover change in the Yellow River Delta and *SAV* is sensitive to environmental change in rivers and sea, while *CAV* is sensitive to environmental change in industrial and urban areas.

1. Introduction

One of the major applications of remotely sensed data obtained from earth-orbiting satellites is change detection (Anderson 1977, Nelson 1983). Change detection, defined as the process of identifying differences in the state of an object or phenomenon by observing it at different times (Singh 1989), is useful in extracting environmental changes.

Many change detection approaches have been developed since the 1970s. They include univariate image differencing (Weismiller *et al.* 1977), image ratioing (Todd 1977), post-classification comparison (Weismiller *et al.* 1977), direct multidate classification (Weismiller *et al.* 1977), vegetation index differencing (Tucker 1979), principal component analysis (Byrne *et al.* 1980), background subtraction (Ballard and Brown 1982), image regression (Singh 1986), and fuzzy set operation (Gong 1993).

Remote sensing has been used to estimate the extent of specific land cover types and to detect changes in land cover that occurred in the past. For instance, Hall *et al.* (1991) detected large-scale patterns of forest succession. Bauer *et al.* (1994) detected forest cover in Minnesota, USA. Stone *et al.* (1994) mapped the vegetation of South America. Fuller *et al.* (1994) detected changes in land cover of Great Britain. Jensen *et al.* (1995) detected inland wetland changes in the Everglades Water Conservation Area in Florida, USA. Miller *et al.* (1998), Bryant *et al.* (1993) and

International Journal of Remote Sensing
ISSN 0143-1161 print/ISSN 1366-5901 online © 2002 Taylor & Francis Ltd
http://www.tandf.co.uk/journals
DOI: 10.1080/01431160110106041

Bryant and Birnie (1991) used Landsat data to estimate vegetation types and wildlife habitats and to detect changes in land cover in the Northern Forest region of Vermont, New Hampshire, and western Maine, USA. Sobrino and Raissouni (2000) monitored changes in land cover of Morocco. Fung and Siu (2000) detected changes in land cover of Hong Kong.

In this paper, we propose a curve-theorem based approach. It is successfully used to extract environmental changes from NDVI data of Landsat MSS images on 1 December 1976 and 3 December 1988 of the Yellow River Delta.

2. Study area

The Yellow River is the second longest river in China and the highest silt-content river in the world. Since the Yellow River took the Daqing river as its course and flowed through Lijin county into the Bohai Sea in 1855, the tail channel of the Yellow River has swung north and south and changed its course over 50 times, taking Ninghai of Kenli county as the central axis. The swinging and silting up has created the Yellow River Delta. The delta is located at the mouth of Bohai Bay and Laizhou Bay (37°20′–38°10′N and 118°7′–119°10′E).

Rapid economic development and the growth of urban population on the Yellow River Delta began with the development of the petroleum industry. Since the Dongying municipality was established in 1983, a new prospect for oil production has been opened up, which includes two major urban districts, namely Dongying district and Hekou district. A petrochemical base for Shandong Province is being developed on the delta. The development of the oil field and petrochemical industry has promoted the development of enterprises in villages and towns, and the construction of infrastructures such as transportation systems, power stations and communication systems.

3. Methods

3.1. *The curve theorem in the plane and the approach for change detection*

3.1.1. *The curve theorem*

Let k: $\{S_0, S\} \rightarrow \Re$ be continuous. Then there is a curve, L: $\{S_0, S\} \rightarrow \Re^2$

parameterized by arc-length, whose curvature at s is $k(s)$ for all $s \in \{S_0, S\}$. Moreover, if L_1 and L_2 are two such curves, then $L_1 = \alpha L_2$ where α is some proper Euclidean motion that is a translation followed by a rotation (Spivak 1979).

3.1.2. *The theoretical expression of the approach*

According to the curve theorem, the overall difference between the two plane curves can be simulated as follows (Yue and Ai 1990, Yue 1994):

$$CD = \frac{1}{S - S_0} \int_{S_0}^{S} ((L_1(S_0) - L_2(S_0))^2 + (\alpha_1(s) - \alpha_2(s))^2 + (k_1(s) - k_2(s))^2) ds \qquad (1)$$

where $k_i(s)$ and $\alpha_i(s)$ are the curvature and slope of the plane curve, L_i, respectively; and $L_i(S_0)$ is the initial value ($i = 1,2$).

It can be proved (Yue *et al.* 1999, Yue and Zhou 1999) that $CD(L_1, L_2)$ has the following three properties: (a) $CD(L_1, L_2) \geqslant 0$; $CD(L_1, L_2) = 0$ if and only if $L_1 = L_2$; (b) $CD(L_1, L_2) = CD(L_2, L_1)$; (c) $CD(L_1, L_3) \leqslant CD(L_1, L_2) + CD(L_2, L_3)$. In functional analysis, $CD(L_1, L_2)$ is measure of distance in metric space of curves (Taylor 1958).

If curves L_i could be simulated as:

$$y = f_i(x) \tag{2}$$

then, α_i and k_i can be respectively formulated as:

$$\alpha_i(x) = \frac{df_i(x)}{dx} \tag{3}$$

$$k_i(x) = \frac{d\alpha_i(x)}{dx}(1+\alpha_i^2(x))^{-3/2} \tag{4}$$

$$ds = (1+\alpha^2(x))^{1/2}dx \tag{5}$$

where x is abscissa and s is arc length.

Suppose that curve $f_2(x)=0$ is considered as an intended-goal-functio n and $f_1(x)$ is an arbitrary function. For $f_1(x)>0$, the better the situation, the longer the distance is from the straight line $f_2(x)=0$. The general index can be formulated as:

$$CD = \frac{1}{X-X_0}\int_{X_0}^{X}(\alpha_1^2(x)+\kappa_1^2(x)+f_1^2(X_0))(1+\alpha_1^2(x))^{1/2}dx \tag{6}$$

where $CD \geqslant 0$; $CD=0$ is the worst situation and the biggest CD is the optimum situation.

3.1.3. *The application expression of the approach*

In this paper, suppose that sequenced data can be expressed in terms of row x and column y as well as time t:

$$V(t) = \begin{bmatrix} v(1,1,t) & v(1,2,t) & \cdots & v(1,Y,t) \\ v(2,1,t) & v(2,2,t) & \cdots & v(2,Y,t) \\ \cdots & \cdots & \cdots & \cdots \\ v(X,1,t) & v(X,2,t) & \cdots & v(X,Y,t) \end{bmatrix} = [\,v(x,y,t)\,]_{X\times Y} \tag{7}$$

where $V(t)$ is the tth layer of the three-dimensional matrix ($t=1,2,...,T$); X is the maximum row number, Y is the maximum column number and T is the maximum value of the time variable. Then, the curve-theorem based approach, which can be formulated as follows in terms of the average in each column, consists of a nonlinear transformation, $SAV(y,t)$, a nonlinear transformation $CAV(y,t)$, and a general index $CD(t)$:

$$SAV(y,t) = \frac{1}{X}\sum_{x=1}^{X} ABS(v(x+1,y,t)-v(x,y,t)) \tag{8}$$

$$CAV(y,t) = \frac{1}{X}\sum_{x=1}^{X}\frac{v(x+2,y,t)-2v(x+1,y,t)+v(x,y,t)}{(1+(v(x+1,y,t)-v(x,y,t))^2)^{3/2}} \tag{9}$$

$$CD(t) = \frac{1}{Y}\sum_{y=1}^{Y}(SAV^2(y,t)+CAV^2(y,t)+AV^2(y,t))(1+SAV^2(y,t))^{1/2} \tag{10}$$

where $AV(y,t)=1/X\,\Sigma_{x=1}^{X}v(x,y,t)$ is an average value in terms of column; $SAV(y,t)$ is an average slope in terms of column; $ABS(number)$ represents the absolute value of the *number*; $CAV(y,t)$ is an average curvature in terms of column.

3.2. *NDVI*

Over the past 20 years, a number of vegetation indices have been developed to aid the interpretation of remotely sensed data (Bouman 1992, Hurcom and Harrison 1998). The most popular vegetation index (Schowengerdt 1997, Purevdorj *et al.* 1998) is the Normalized Difference Vegetation Index (NDVI):

$$NDVI = \frac{\lambda_{NIR} - \lambda_{RED}}{\lambda_{NIR} + \lambda_{RED}} \tag{11}$$

where λ_{RED} is the spectral reflectance of the visible red band; λ_{NIR} is the spectral reflectance of the near-infrared band. NDVI has been widely used in describing relationships between vegetation characteristics such as above-ground biomass, green biomass and chlorophyll content (Tucker 1985).

To make it easy to calculate the general index, we transform NDVI into:

$$v(x,y,t) = \frac{1 + NDVI(x,y,t)}{2} \tag{12}$$

where $0 \leqslant v(x,y,t) \leqslant 1$; $t = 1$ and 2 respectively correspond to 1 December 1976 and 3 December 1988; (x,y) represents the pixel location.

3.3. *The comparability of Landsat MSS data and Landsat TM data*

In the pattern decomposition method presented by Muramatsu *et al.* (2000), the spectral response patterns for each pixel in an image are decomposed into three components using three standard spectral patterns normalized to unity. The three standard spectral patterns are determined to correspond to water, vegetation and soil. In spite of the differences in measured band number and wavelength, MSS data can be analyzed in the same parameter space as TM data. The difference in classification results between TM and MSS was 1.8%.

Our sampling analysis also found that TM and MSS gave similar classifications:

(a) The area, $449 \leqslant x \leqslant 450$ and $1296 \leqslant y \leqslant 1300$, is covered by *imperata cylindrica* and is located in the core region of the Yellow River Delta Natural Conservation Area. The linear regression equation is,

$$NDVI_v^{TM} = 0.46\, NDVI_v^{MSS} - 0.08 \tag{13}$$

The correlation coefficient is 0.71.

(b) The area, $2813 \leqslant x \leqslant 2814$ and $606 \leqslant y \leqslant 610$, is a residential quarter that remained the same between 1976 and 1988 according to our investigation on site. The linear regression equation of the corresponding NDVI data is:

$$NDVI_r^{TM} = 0.58\, NDVI_r^{MSS} + 0.02 \tag{14}$$

The correlation coefficient is 0.75.

(c) The area, $2974 \leqslant x \leqslant 2975$ and $1888 \leqslant y \leqslant 1892$, is a sandy area that had almost no land cover change during the 12 years because of the tides. The linear regression equation is:

$$NDVI_s^{TM} = 0.43\, NDVI_s^{MSS} - 0.01 \tag{15}$$

The correlation coefficient is 0.80.

(d) The area, $3136 \leqslant x \leqslant 3137$ and $2996 \leqslant y \leqslant 3000$, is located at the Bohai Sea, which is relatively far away from the changed continental river system. The linear regression equation is:

$$NDVI_w^{TM} = 0.52\, NDVI_w^{MSS} + 0.09 \tag{16}$$

The correlation coefficient is 0.78.

4. Materials and results

The input for the curve-theorem based approach is two visualized algebraic matrixes (figures 1 and 2). Each scene has 14 057 576 pixels that are divided into 4582 rows and 3068 columns. The size of each pixel is $30 \times 30\,m^2$. The output

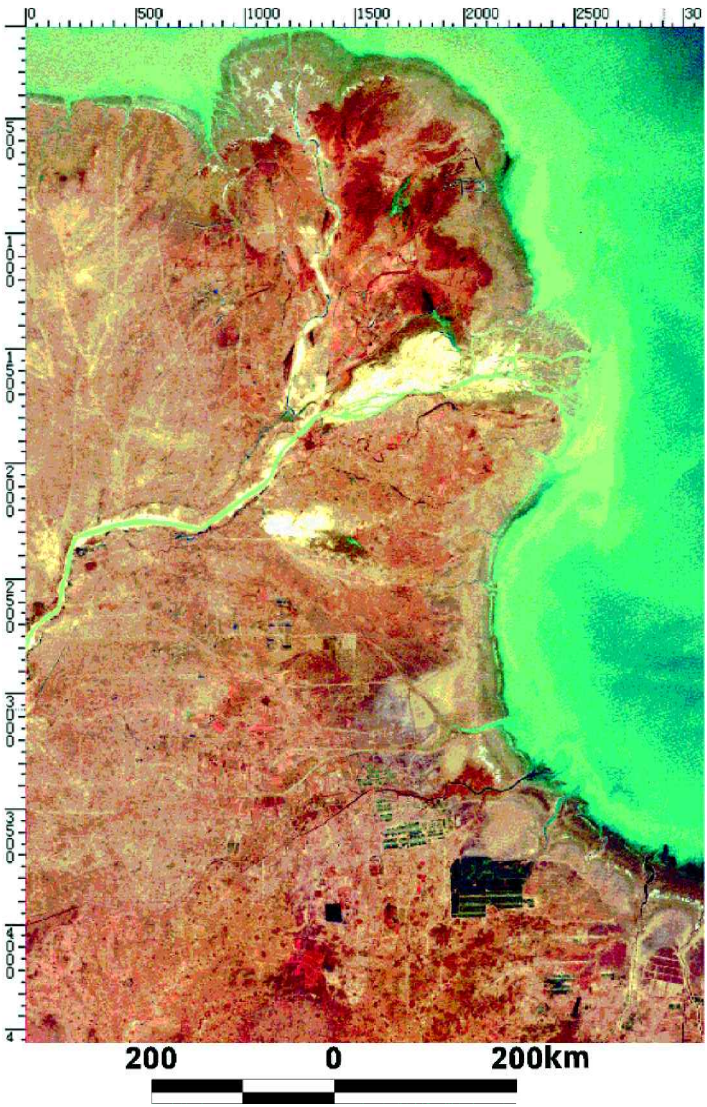

Figure 1. A visualization of the algebraic matrix transformed from the Landsat image acquired on 1 December 1976 over the Yellow River Delta.

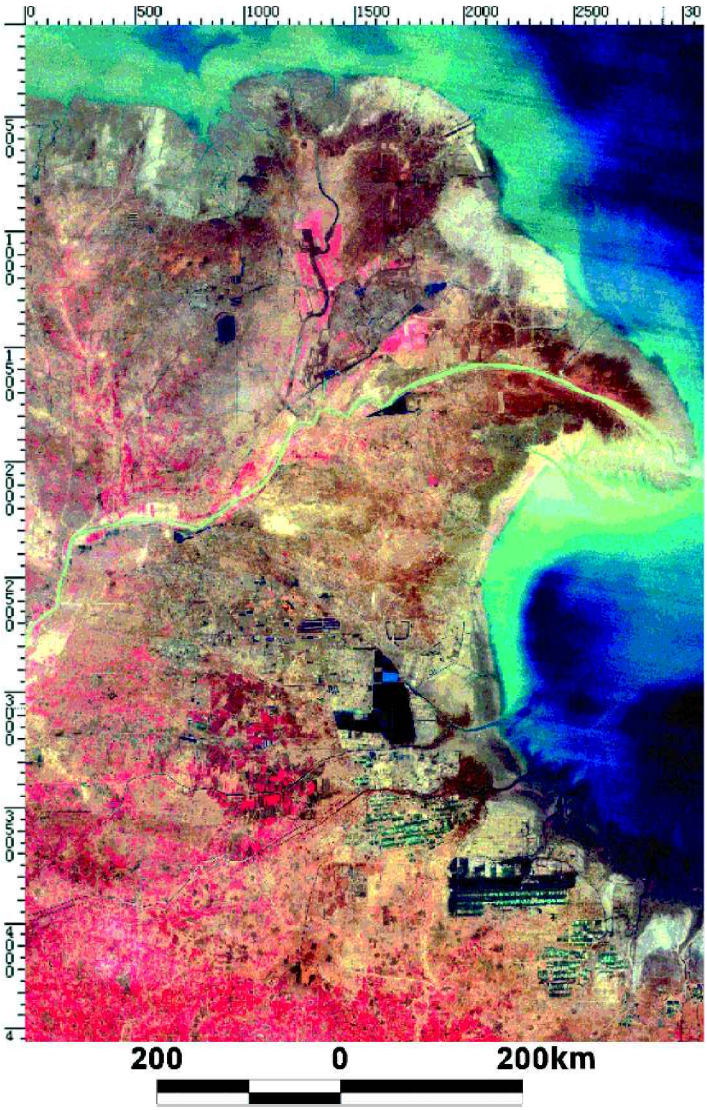

Figure 2. A visualization of the algebraic matrix transformed from the Landsat image acquired on 3 December 1988 over the Yellow River Delta.

includes the general index *CD*, the nonlinear transformation *SAV*, and the nonlinear transformation *CAV*.

According to the research results from Muramatsu *et al.* (2000) and our samples, if the environment had no change between 1976 and 1988, the transformation curves should have the same progressive increase and convexity; if the transformation curves have different progressive increase or convexity between 1976 and 1988, then the environment must have undergone substantial changes. In other words, in addition to extracting environmental changes in the whole area of the Yellow River Delta by comparing the general indexes, local environmental changes can be found by comparing the progressive increase or the convexity between transformation curves.

Because the calculation results in terms of the average in each row not provide us information change, we only report the results in terms of average in each column.

4.1. *The general index*

Our results indicate that $0.1554 \leqslant AV(y,t) \leqslant 0.4799$, $0.0119 \leqslant SAV(y,t) \leqslant 0.0266$, and $-1.53E-05 \leqslant CAV(y,t) \leqslant 1.14E-05$. The general index in terms of average in each column can be simplified as:

$$CD(t) \approx \frac{1}{Y} \sum_{y=1}^{Y} ((AV(y,t))^2 + (SAV(y,t))^2)(1 + (SAV(y,t))^2)^{1/2} \tag{17}$$

By applying CD to the two images, we obtain $CD(1) = 0.1448$, $CD(2) = 0.2001$. Obviously, from 1976 to 1988, NDVI was increased in the Yellow River Delta. We should note that if vegetation cover has no change, $CD(1)$ should be greater than $CD(2)$ according to the sample statistics presented earlier.

4.2. *The nonlinear transformation SAV*

$SAV(y,t)$ provides us with a rich amount of knowledge on change along rivers as seen in figure 3 and figure 4:

- when $184 \leqslant y \leqslant 481$, which corresponds to the Zhanli river, $SAV(y,1)$ decreases progressively and $SAV(y,2)$ increases progressively;
- when $1156 \leqslant y \leqslant 1435$, which corresponds to the old course of the Yellow River, $SAV(y,1)$ is concave and $SAV(y,2)$ is close to a straight line;
- when $2088 \leqslant y \leqslant 2330$, which corresponds to the coastal boundary area where the west side of the Yellow River Delta meets with the Bohai Sea, $SAV(y,1)$ is convex and $SAV(y,2)$ is concave;
- when $2463 \leqslant y \leqslant 2950$, in which $y = 2463$ is the mouth of the Yellow River flowing into the Bohai Sea in 1976 and $y = 2950$ is the mouth of the Yellow River flowing into the Bohai Sea in 1988, $SAV(y,1)$ increases progressively and $SAV(y,2)$ decreases progressively.

In other words, $SAV(y,1)$ and $SAV(y,2)$ have a greater difference of progressive increase and convexity in these areas. This indicates that the ecological environment of the areas along the rivers has been greatly changed since 1976. According to our field visit, boats were able to sail in the Zhanli river in 1976 because there was water from the Yellow River flowing into the Bohai Sea through the Zhanli river, while there was no water from the Yellow River flowing into the Bohai Sea through the Zhanli river in 1988. The Zhanli river became a drainage canal because the connection between the Zhanli river and the Yellow River had been artificially cut off. There was some water from the Yellow River flowing into the Bohai Sea through the old course of the Yellow River in 1976, while some parts of the old course of the Yellow River had become farmland and *phragmitas communis* Trin. had become established *Trin. Ex Steud.* Land. There was a heavy red tide in the Bohai Sea near the Yellow River Delta in 1988 while there was almost none in 1976.

4.3. *The nonlinear transformation CAV*

From $CAV(y,2)$ as seen in figure 5 we find that:

- when $628 \leqslant y \leqslant 784$, where the two biggest urban districts of the Dongying municipality, Dongying district and Hekou district, as well as many bigger towns of the Dongying municipality such as Luozheng, Niuzhuang, Jixian,

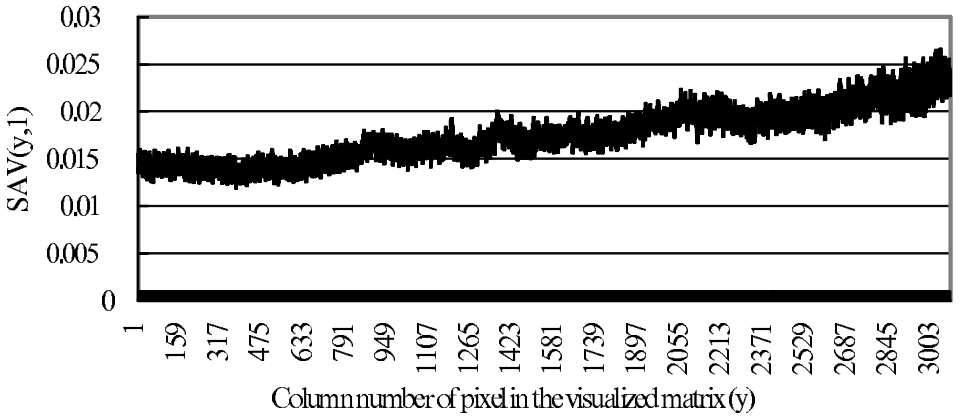

Figure 3. $SAV(y,1)$, a nonlinear transformation of NDVI in 1976 (in terms of average of each column).

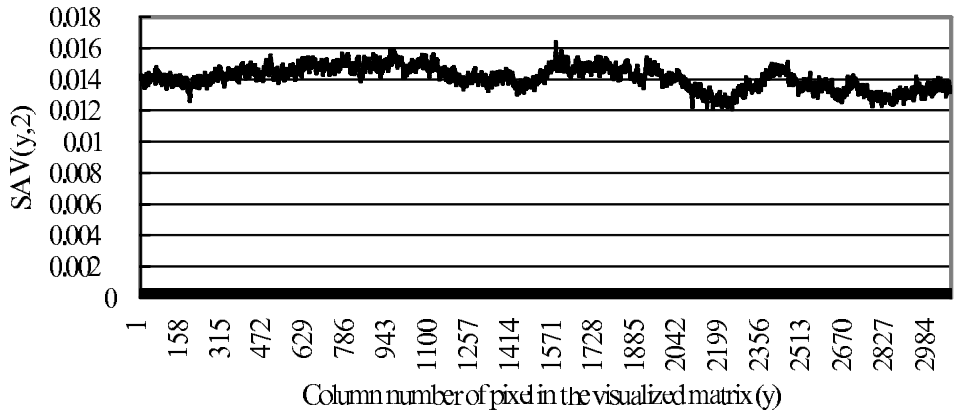

Figure 4. $SAV(y,2)$, a nonlinear transformation of NDVI in 1988 (in terms of average of each column).

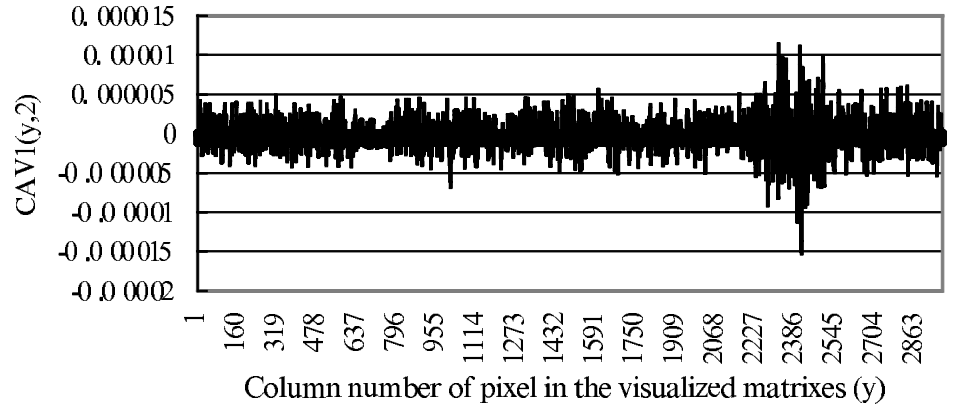

Figure 5. $CAV(y,2)$, a nonlinear transformation of NDVI in 1988 (in terms of average of each column).

Kenli, Gaogai, Chenguan, Daying, Daozhuang and Xiying, are located, the range of CAV is $-1.4993E-06 \leqslant CAV1(y,2) \leqslant 1.8278E-06$. In other words, the values in this range are very small and have a rather even distribution.

- when $2167 \leqslant y \leqslant 2454$, where the biggest oil extraction area of the Gudao oilfield is located, the range of CAV is $-1.531E-05 \leqslant CAV1(y,2) \leqslant 1.141E-05$. In other words, the biggest and smallest values of CAV both occur in this range and a sharp change exists.

5. Conclusions

Environmentally, from 1976 to 1988, with the rapid growth of the Shengli oil field and especially the great development of the Gudao oilfield, water areas in the Yellow River Delta including the rivers and the Bohai Sea have been heavily polluted; the vegetation cover near the Gudao oilfield has been greatly destroyed. But development of the Shengli oil field and related industries has promoted economic development in the local region and improvement of the vegetation cover in the agricultural area south of the Yellow River generally, despite the complete destruction of the biggest *Robinia pseudoacacia L.* woodland in this area. Methodologically, the general index CD gives us an overall view on vegetation cover change. The SAV provides us with useful information on environmental changes of rivers. CAV is capable of highlighting the location of industrial and urban areas.

Acknowledgments

This research was supported by the Knowledge-Innovation Project of the Chinese Academy of Sciences (kzcx2-308-02) and by the Knowledge-Innovation Project of the Institute for Geographical Science and Resources of the Chinese Academy of Sciences (CX10G-D00-02). Mr Hai Jin Li helped in the preparation of figures.

References

Anderson, J. R., 1977, Land-use change analysis using sequential aerial photography and computer technique. *Photogrammetric Engineering and Remote Sensing*, **46**, 1447–1464.

Ballard, D. H., and Brown, N. A., 1982, *Computer Vision* (New Jersey: Prentice Hall).

Bauer, M. E., Burk, T. E., Ek, A. R., Coppen, P. R., Lime, A. D., Walsh, T. A., Walters, D. K., Befort, W., and Heinzen, D. F., 1994, Satellite inventory of Minnesota forest resources. *Photogrammetric Engineering and Remote Sensing*, **60**, 287–298.

Bouman, B. A., 1992, Accuracy of estimating the Leaf Area Index from vegetation indices derived from crop reflectance characteristics, a simulation study. *International Journal of Remote Sensing*, **13**, 3609–3084.

Bryant, E. S., and Birnie, R. W., 1991, Landsat satellite mapping of selected biomes, wildlife habitats, and clearcuts in the Northern Forest Lands: a pilot study. Report for the Appalachian Mountain Club, Gorham, NH.

Bryant, E. S., Birnie, R. W., and Kimball, K. D., 1993, A practical method of mapping forest change over time using Landsat MSS data: a case study from central Maine. *Proceedings of 25th International Symposium, Remote Sensing and Global Environmental Change*, Graz, Austria, 4–8 April (Ann Arbor: ERIM), pp.469–480.

Byrne, G. F., Crapper, P. F., and Mayo, K. K., 1980, Monitoring land cover change by principal component analysis of multitemporal Landsat data. *Remote Sensing of Environment*, **10**, 175–184.

Fuller, R. M., Groom, G. B., and Jones, A. R., 1994, The land cover map of Great Britain: an automated classification of Landsat Thematic Mapper data. *Photogrammetric Engineering and Remote Sensing*, **60**, 553–562.

Fung, T., and Siu, W., 2000, Environmental quality and its changes, an analysis using NDVI. *International Journal of Remote Sensing*, **21**, 1011–1024.

GONG, P., 1993, Change detection using principal component analysis and fuzzy set theory. *Canadian Journal of Remote Sensing*, **19**, 22–29.

HALL, F. G., BOTKIN, D. B., STREBEL, D. E., WOODS, K. D., and GOETZ, S. J., 1991, Large-scale patterns of forest succession as determined by remote sensing. *Ecology*, **72**, 628–640.

HURCOM, S. J., HARRISON, A. R., 1998, The NDVI and spectral decomposition for semi-arid vegetation abundance estimation. *International Journal of Remote Sensing*, **19**, 3109–3125.

JENSEN, J. R., RUTCHEY, K., KOCH, M. S., and NARUMALANI, S., 1995, Inland wetland change detection in the Everglades Water Conservation Area 2A using a time series of normalized remotely sensed data. *Photogrammetric Engineering and Remote Sensing*, **61**, 199–209.

MILLER, A. B., BRYANT, E. S., and BIRNIE, R. W., 1998, An analysis of land cover changes in the Northern Forest of New England using multitemporal Landsat MSS data. *International Journal of Remote Sensing*, **19**, 245–265.

MURAMATSU, K., FURUMI, S., FUJIWARA, N., HAYASHI, A., DAIGO, M., and OCHIAI, F., 2000, Pattern decomposition method in the albedo space for Landsat TM and MSS data analysis. *International Journal of Remote Sensing*, **21**, 99–119.

NELSON, R. F., 1983, Detecting forest canopy change due to insect activity using Landsat MSS. *Photogrammetric Engineering and Remote Sensing*, **49**, 1303–1314.

PUREVDORJ, T., TATEISHI, R., ISHIYAMA, T., and HONDA, Y., 1998, Relationships between percent vegetation cover and vegetation indices. *International Journal of Remote Sensing*, **19**, 3519–3535.

SCHOWENGERDT, R. A., 1997, *Remote Sensing: Models and Methods for Image Processing* (London: Academic Press).

SINGH, A., 1986, Change detection in the tropical forest environment of north eastern India using Landsat. In *Remote Sensing and Tropical Land Management*, edited by M. J. Eden and J. T. Parry (London: John Wiley & Sons), pp.237–254.

SINGH, A., 1989, Digital change detection techniques using remotely-sensed data. *International Journal of Remote Sensing*, **10**, 989–1003.

SOBRINO, J. A., and RAISSOUNI, N., 2000, Toward remote sensing methods for land cover dynamic monitoring: application to Morocco. *International Journal of Remote Sensing*, **21**, 353–366.

SPIVAK, M., 1979, *A Comprehensive Introduction to Differential Geometry* (Houston, Texas: Publish or Perish, Inc).

STONE, T. A., SCHLESINGER, P., HOUGHTON, R. A., and WOODELL, G. M., 1994, A map of the vegetation of South America based on satellite imagery. *Photogrammetric Engineering and Remote Sensing*, **60**, 541–551.

TAYLOR, A. E., 1958, *Introduction to Functional Analysis* (New York: John Wiley & Sons, Inc).

TODD, W. J., 1977, Urban and regional land use change detected by using Landsat data. *Journal of Research by the US Geological Survey*, **5**, 527–534.

TUCKER, C. J., 1979, Red and photographical infrared linear combinations for monitoring vegetation. *Remote Sensing of Environment*, **8**, 127–150.

TUCKER, C. J., 1985, Satellite remote sensing of total herbaceous biomass production in the Senegalese Sahel: 1980–1984. *Remote Sensing of Environment*, **17**, 233–249.

WEISMILLER, R. A., KRISTOF, S. J., SCHOLZ, D. K., ANUTA, P. E., and MOMEN, S. A., 1977, Change detection in coastal zone environments. *Photogrammetric Engineering and Remote Sensing*, **43**, 1533–1539.

YUE, T. X., and ZHOU, C. H., 1999, An approach of differential geometry to data mining. *Towards Digital Earth: Proceedings of the International Symposium on Digital Earth, held in Beijing, 29 November–2 December 1999* (Beijing: Science Press), pp.789–802.

YUE, T. X., HABER, W., GROSSMANN, W. D., and KASPERIDUS, H. D., 1999, A method for strategic management of land. In *Environmental Indices: Systems Analysis Approaches*, edited by Y. A. Pykh, D. E. Hyatt and R. J. M. B. Lenz (London:EOLSS Publishers Co Ltd.), pp.181–201.

YUE, T. X., 1994. *Systems models for land management and real estate evaluation* (Beijing: China Society Press, in Chinese).

YUE, T. X., and AI, N. S., 1990. A morphological mathematical model for cirques. *Glaciology and Cryopedology*, **12**, 227–234 (in Chinese).